*Int. J. Mol. Sci.* **2007**, *8*, 1-12

International Journal of
**Molecular Sciences**
**ISSN 1422-0067**

www.mdpi.org/ijms/

# Self-assembly and Fractal Feature of Chitosan and Its Conjugate with Metal Ions: Cu (II) / Ag (I)

**Yi Hu [1], Yangzhe Wu [1], Jiye Cai [1,*], Yufeng Ma [2], Bin Wang [1], Ke Xia [1] and Xiaoqing He [1]**

[1] College of Life Science and Technology, Jinan University, Guangzhou 510632, P.R. China
E-mail: jerry_wyzhe@hotmail.com, luly_hu@yahoo.com.cn

[2] School of Pharmaceutical Sciences, Southern Medical University, Guangzhou 510515, P.R. China
E-mail: happymyf@tom.com

* Author to whom correspondence should be addressed; E-mail: tjycai@jnu.edu.cn, Fax (Tel): + 86-20-8522-3569. Postal address: Chemistry Department, Jinan University, Guangzhou 510632, P.R. China

*Received: 10 Novemver 2006 / Accepted: 16 January 2007 / Published: 24 January 2007*

---

**Abstract:** In this paper, we investigated the self-assembly and fractal feature of chitosan and Ag (I), Cu (II)-chitosan due to the theoretical and practical importance of chitosan in biomedical engineering, biomaterials and environmental sciences etc. The self-assembly and fractal structures of chitosan and Ag (I), Cu (II)-chitosan were observed using atomic force microscope (AFM), and the fractal dimensions of chitosan and Ag (I)-chitosan were calculated. The results indicate that their fractal dimension is approximate 2 and relates with the accumulation degree: the fractal dimension decreases with the accumulation degree increases. In addition, a new self-assembly strategy was presented to study the lyotropic liquid crystals (LLC) of chitosan and the formation mechanism of LLC was primarily analyzed and discussed. All of these results are valuable for the structure/function relationship study of chitosan and useful for application in biomedical materials.

**Keywords:** Chitosan; Self-assembly; Fractal; Liquid crystal; Atomic force microscope

---

## 1. Introduction

The theory of self-assembly and fractal has been extensively applied in structures/function studying of biomacromolecules [1-9], which opens many new opportunities for us to understand the

physicochemical properties of biomacromolecules. Moreover, the study of self-assembly and fractal feature of chitosan is of great theoretical and practical importance [15-18]. Molecular self-assembly offers a means of spontaneously forming complex and well-defined structures from simple components [10]. The technology of self-assembled monolayer (SAM) provides a convenient way to construct perfect interface at molecular level [19, 20]. Recently, SAM has become a hotspot studying due to its excellent homogeneity and stability over LB film. On the other hand, Fractal theory which was brought forward by Mandelbrot in 1975 is so pervasive in nature [25] and has been extensively applied in many subjects including molecular biology [26-30] such as structure/function relationship study of biomacromolecules.

Chitosan is a kind of unique natural alkalescence polysaccharide molecule that consists of double helix structure, and it's the structural unit is chitobiose (Figure 1). The molecular weight of chitosan can exceed a million Daltons. Chitosan film is easily prepared due to its physicochemical properties such as adhesion property, permeability and tensile strength. Up to now, biocompatible chitosan film has been extensively applied as biomedical materials [11-14] and there have been many relative reports such as artificial skin [21-23] and artificial kidney [24].

In addition, the intra-structure of macromolecular compound is very complex, and exist crystal phase region and non-crystal phase region. The crystallinity is the weight percent of crystal phase region, and the stable physicochemical properties of chitosan should be ascribed to its high crystallinity, which increases with the de-acetyl degree increasing. In 1982, Ogura firstly reported the lyotropic liquid crystals (LLC) of chitosan, after that, the studies on liquid crystals of chitosan and its ramification became extensive [31, 32].

In this paper, we investigated chitosan molecule chain, lyotropic liquid crystals of chitosan, the self-assembly and fractal feature of chitosan and chitosan/metal ions based on atomic force microscope (AFM), and the results provide us some valuable data, new evidence and inspiration to understand the self-assembly and fractal theory or phenomenon that present at nanometer scale world. Furthermore, we can obtain some useful evidences and novel views to investigate the structure/function relationship of chitosan which is related to their active bio-function in practice.

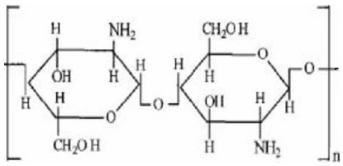

**Figure 1.** Structural illustration of chitosan.

## 2. Results and discussion

### *2.1 Chitosan molecule chain*

The molecular weight of chitosan is very large (exceeds a million Daltons), so single chitosan molecular image is possibly acquired in air. Here, chitosan molecular chain was clearly visualized (Figure 2a, 2b). The size of single linear chitosan molecules is of importance for us understanding the interaction between chitosan molecules, so, those linear molecules that look like single, not complex, chitosan molecule chain were measured using AFM processing software (Figure 2c), then a statistical

analysis was performed, and the results indicated that the length of chitosan molecules is 971.71±111.40 nm, the mean diameter (Full Width at Half Maximum, FWHM) is 21.42 nm, the mean height is 2.20 nm, and their standard deviation (*S*) are 3.70 nm and 0.97 nm, respectively. After considering the stretch effect of tip, the sizes of breadth and height of molecular chain approximate to the theoretical value (approximately 1 nm), so the molecular chain in Figure 2 measured using short white lines (lines A, B and C) should be single chain. On the other hand, the molecular chains of chitosan easily accumulate and present dendritic structures (arrows in Figure 2b), and as the large black arrow showed in Figure 2b, this location should be probably consisted of four single chitosan molecular chains, and here, the intermolecular and intramolecular hydrogen bond played a key role in chain enwinding. In addition, there are many spherical particles in Figure 2, which should be impurity that results from chitosan sample itself, or chitosan fragments.

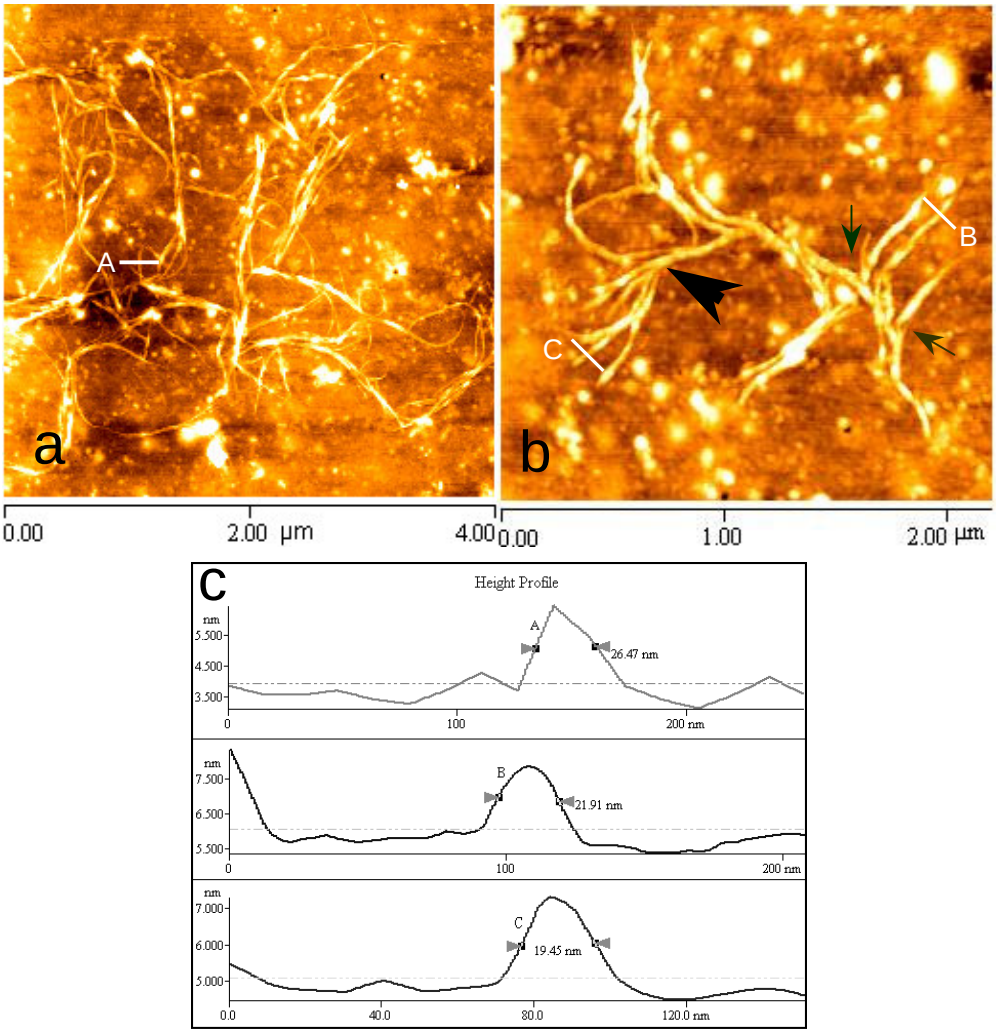


**Figure 2.** Morphological image of chitosan molecule chain (a, b). The molecular chains of chitosan accumulate to present dendritic structures (blue arrows). (c) The height profiles A, B and C were generated along the white lines A, B and C shown in Figure a and Figure b, respectively. The FWHM in Figure c are 26.47 nm (line A), 21.91 nm (Line B) and 19.45 nm (Line C), and the heights are 2.384 nm, 1.694 nm and 2.156 nm.

*2.2 Chitosan film*

Figure 3 is AFM images of chitosan film with different concentration: 1.0 mg/ml (3a) and 2.5 mg/ml (3b). The film in Figure 3 presents mesh structure, which is consisted of meshes with 80 nm-110 nm in diameter (blue annuluses in Figure 3a), and the distance between meshes is 40.95±6.45 nm; however, the mesh diameter in Figure 3b is 280 nm~440 nm, and the distance between meshes is 222.79±58.78 nm, which indicate that the size of the mesh structures of chitosan film increases with the concentration (chitosan) increasing, in this way, the mesh structures of chitosan film can stay in a low free energy state (the mesh structures could form when chitosan concentration is appropriate). The chitosan film with mesh structure should be ascribed to single macromolecular chain of chitosan enwinding with each other. According to the height profile (3c, 3d) that generate along lines in Fig (3a, 3b), the thickness of film could be measured. In Figure c and d, the difference between the two arrowheads (upper arrowhead points to mean thickness line, and lower arrowhead points to substrate) is 6.342 nm and 12.89 nm, respectively, which are the thickness of chitosan film. The statistic analytic results indicate that mean thickness of film is 6.45 nm (3a) and 11.65 nm (3b), and the average rough (Ra) is 1.74 nm (3a) and 5.53 nm (3b), which increase with the concentration increases.

Chitosan film has many implications in practice such as bandages, which can be used as coagulant material to rapidly clot blood and stop the bleeding. On the other hand, the air permeability is of importance for chitosan film using as haemostatic material, the upper results indicated that the air permeability of chitosan film can be regulated by changing the size of mesh structures, which can be attained via altering the chitosan concentration.

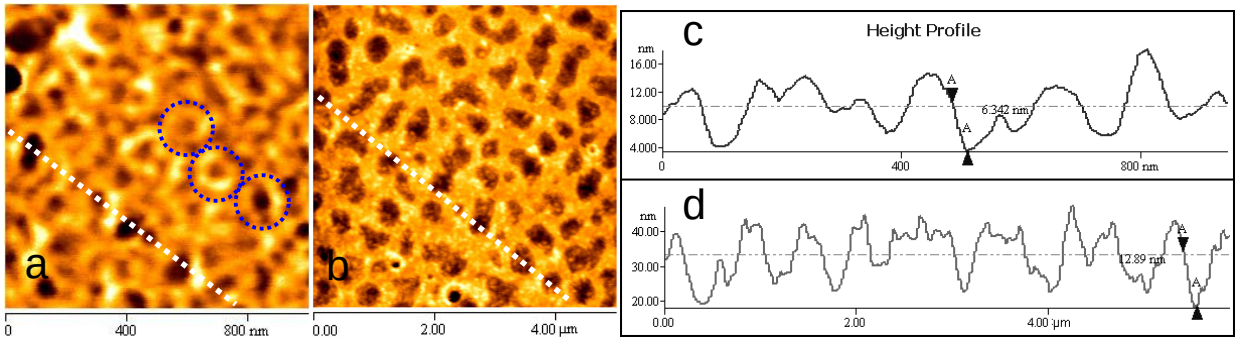


**Figure 3.** AFM images of chitosan film with mesh structure (a, 1.0 mg/ml; b 2.5 mg/ml). Figure c and d are height profile generated along the white broken lines in Figure a and b, respectively. The average rough (Ra) is 1.74 nm (a) and 5.53 nm (b), and the mean thickness of film is 6.45 nm (a) and 11.65 nm (b) according to statistic analysis.

*2.3 Fractal structures of chitosan*

Here, the fractal structure of chitosan on mica was analyzed by AFM, Figure 4 is the AFM images of colloidal particles (4a) and fractal structures (4b, 4c) of chitosan, which indicate that the fractal growth mode is accordant with the diffusion-limited aggregation (DLA) model of fractal growth (4b', 4c'). The stelliform colloidal particles (blue arrow, 4a) and the stochastic furcated stelliform structure (4b) externalized the self-similarity of fractal structure. As for fractal dimension, the calculated results are 1.977 (4b) and 1.960 (4c). Moreover, the results indicate that the fractal dimension related with the

accumulated degree of colloidal particles: the more compactly the colloidal particles accumulate (4c), the smaller the fractal dimension is. All of these results could provide new evidence and inspiration to understand the fractal theory, and lead us to probe the complex and mysterious fractal phenomenon that presents at nanometer scale world, moreover, we could obtain some useful evidences and novel views to investigate the structure/function relationship of chitosan which is related to their active function in practice.

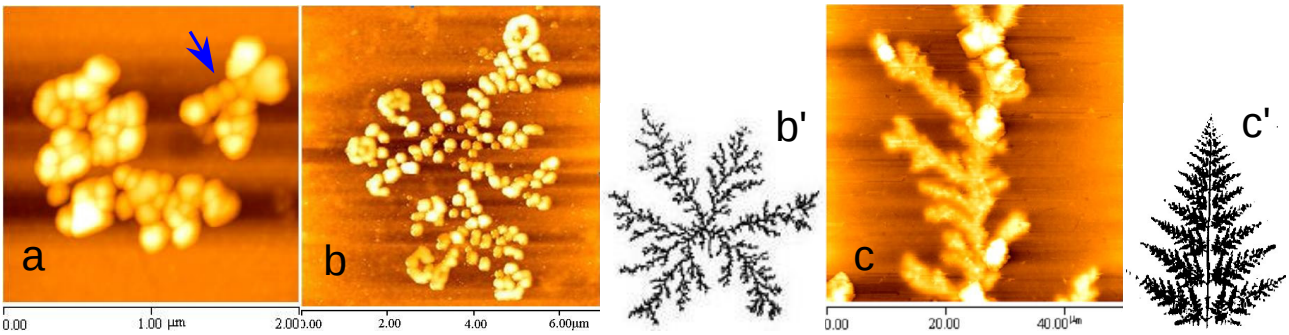


**Figure 4.** Colloidal particles (a) and fractal structure (b, c) of chitosan and their DLA models (b', c'). The fractal dimension is 1.977 (b) and 1.960 (c).

*2.4 Liquid crystal feature of chitosan*

The results indicate that the self-assembly process of chitosan on mica is very interesting due to the interaction between chitosan polycation and positively charged mica. Irregular polygon, hexagon and circular lyotropic liquid crystals (LLC) of chitosan were all visualized at initial time (Figure 5a, 5b). At very low concentration, the chitosan molecules will be dispersed randomly without any ordering. At slightly higher (but still low) concentration, molecules will spontaneously assemble into micelles or vesicles to stay in low free energy state. At higher concentration, the assemblies will become ordered, and the typical phase is a hexagonal columnar phase, where the chitosan molecules form long cylinders that arrange themselves into a roughly hexagonal lattice (Figure 5b). In the experiment, the concentration of chitosan solution (5%) is lower than the saturated concentration (6%, weight ratio) in 36% acetic acid solution, so LLC of chitosan would form when chitosan concentration exceeds the saturated concentration during air-dried process. This stage is a two-phase coexisted region of liquid/isotropy, and aeolotropy region formed circular structures. At the initial time, chitosan micelle accumulated compactly and presented concentric ring-like LLC structures (Figure 5b), however, these concentric ring-like LLC structures turned into hollow ring-like structures at 16 h (Figure 5c). These results probably related with the repulsive interaction between chitosan polycation and positively charged mica, which probably play a very important role during the formation of LLC of chitosan (Figure 5a, 5b), on the other hand, the "water film" in micro-space on sample surface [33] should be the major factor of the formation of the concentric ring-like structures (Figure 5c) due to its lower free energy, and this result also indicates that the LLC of chitosan can not be preserved in air for a long time. Figure 5d is the height profile generated along the broken line in Figure 5b, the diameter is 2.971 µm, and the thickness is 52.34 nm (the difference between two arrowheads in Figure 5d). According to AFM analysis, the diameter distributed between 1.1 µm and 3.5 µm, and the mean height of LLC (Figure 5a) is 44.04±1.9 nm.

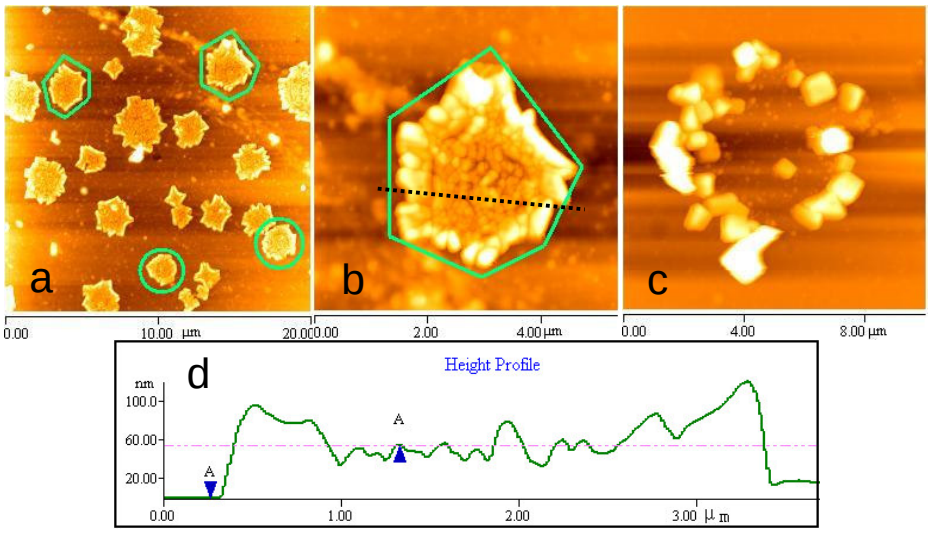


**Figure 5.** The AFM images of lyotropic liquid crystals of chitosan. Figure a, b are images obtained as soon as chitosan dropped on mica; Figure c is the images obtained at 16 h. Figure d is the height profile generated along the broken line in Figure 5b, the diameter is 2.971 µm, and the thickness is 52.34 nm (the difference between two arrowheads in Figure 5d).

To testify the chitosan aggregation in Figure 5 is not spherocrystal but liquid crystal, an X-ray diffraction experiment was performed, and the result was that no diffraction peak of crystal was observed except for dispersion peak of non-crystal (Figure 6).

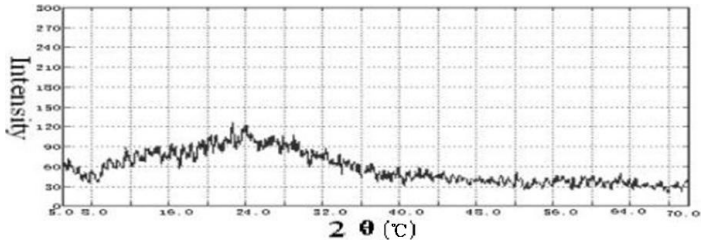


**Figure 6.** The XRD result of solution casting films of chitosan.

*2.5 The self-assembly and fractal feature of Cu (II), Ag (I)-chitosan conjugates*

Firstly, 0.1 mg/ml $Cu(NO_3)_2$ and $AgNO_3$ solution were mixed with 0.1 mg/ml chitosan solution, then the self-assembly nanostructure of chitosan induced by Cu (II) and Ag (I) was studied by AFM. Figure 7a and 7b are self-assembly images of Cu (II)-chitosan conjugate acquired at different time, and the annularly self-assembly structure formed as time passed by (7b). In our experiment, many annulus structures have been observed, and the possible explanation is that the system in Figure 7a is not stable enough; however, annulus structure (30 µm in diameter, Figure 7b) is relatively stable due to the lower free energy compared to Figure 7a.

On the other hand, the stelliform fractal structures of Cu (II)-chitosan conjugate (Figure 7c) and Ag (I)-chitosan conjugate (7d) are accordant with the DLA model (Figure 4b'), and the fractal dimensions are 1.947 (7c) and 1.957 (7d). According to the results, the fractal dimensions of Cu (II), Ag (I)- chitosan conjugate are less than that of chitosan (see Figure 4), and their mean fractal dimensions are

1.952±0.005 (conjugate) and 1.969±0.009 (chitosan), respectively, which indicated that Cu (II), Ag (I) could reduce the fractal dimensions of chitosan fractal structures.

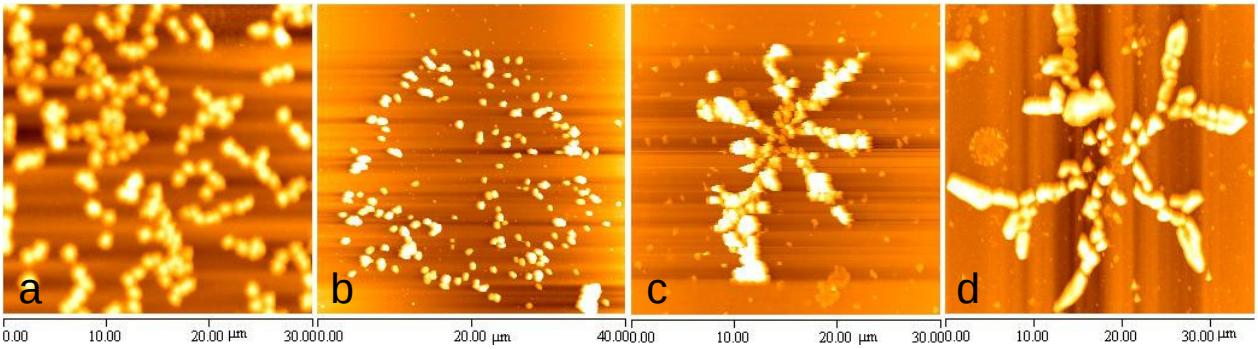


**Figure 7.** The self-assembly images of Cu (II)-chitosan micelle (a, b), the size of micelle in Figure 7a is 1.35µm~1. 85µm in diameter, 290nm~450nm in height, their mean values are 1.52µm and 373 nm, respectively. Figure c and d are fractal structural images of Cu (II), Ag (I)-chitosan aggregates, and the fractal dimensions are 1.947 (c) and 1.957 (d), respectively.

When 1 mg/ml $Cu(NO_3)_2$ and $AgNO_3$ solution were mixed with 0.1 mg/ml chitosan solution, discal structures that accord with the Eden model of fractal (Figure 8c) were observed (Figure 8a, 8b), and the diameter of the "disk" of Cu (II)-chitosan is larger than that of Ag (I)-chitosan: variation from 32 µm (8a) to 4.46µm (8b). Figure 8a' and 8b' are the height profiles of Figure 8a and 8b, respectively, which indicate that the height at edge is higher than that in center. Here, the formation of the discal structure should be ascribed to the destruction of the stable condition of random distribution of Cu (II), Ag (I)-chitosan micelle, and the driving force of micelle aggregates is intermolecular force and electrostatic force. Aggregation growth stopped when a regular "disk" formed because of the space limiting. So, the main agent of the formation of discal structure originated from the surface tension and anisotropy, meanwhile fluctuation also played an important role [34].

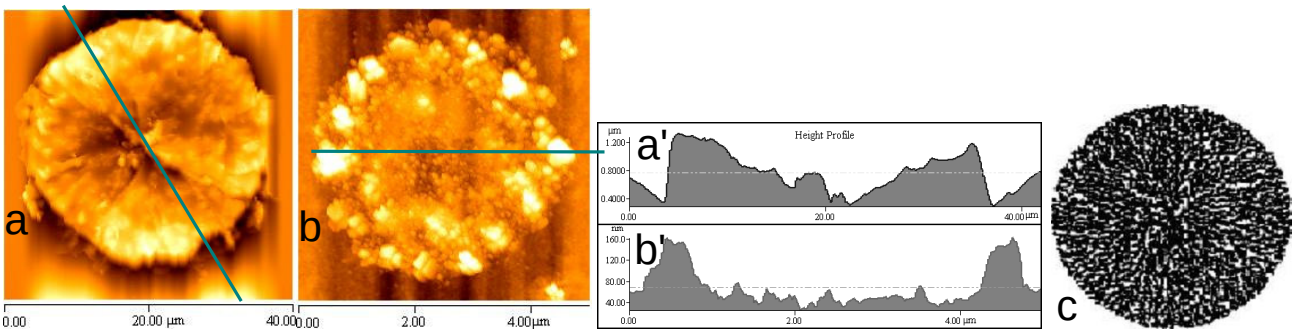


**Figure 8.** Self-assembly discal structures and height profile of conjugates of Cu (II)-chitosan (a) and Ag (I)-chitosan (b). Figure c is the Eden model of fractal.

## 3. Conclusion

In this paper, we investigated chitosan molecular chains, chitosam film, lyotropic liquid crystals (LLC) of chitosan, and the self-assembly and fractal feature of chitosan and the chitosan/metal ions aggregates. According to our investigation and results, we discovered that the molecular chains of chitosan accumulate to present dendritic structures, and the size of chitosan chain is 971.71±111.40 nm

in mean length, 21.42±3.70 nm in mean diameter (FWHM), and 2.20±0.97 nm in mean height. These statistical data approximate to the theoretical value after considering the stretch effect of AFM tip. The self-assembly film of chitason presents mesh structures, whose diameter increases with the concentration increases and the average rough of chitosan film varies in the same way. By adopting a new self-assembly strategy, we discovered the interaction between chitosan polycation and positively charged mica is very interesting and LLC of chitosan that validated by XRD were visualized and a statistical analysis about the size of LLC was then performed. The self-assembly process of LLC of chitosan on positively charged mica was also explained.

As for the fractal feature of chitosan and Ag (I)-chitosan, we calculated their fractal dimensions using the formula [35]: $D=(d^2+1)/(d+1)$, the results indicate that their fractal dimensions are approximate 2 (see Figure 5 and 8), which is accordant with the result of Montembault [18]. Meanwhile, the fractal dimension is related with the accumulation degree: the fractal dimension decreases with the accumulation degree increases (see Figure 5b, 5c and Figure 8c, 8d). According to the results, we find that the fractal structures of Cu (II), Ag (I)-chitosan conjugate is accordant with the DLA model (7c, 7d) and the Eden model (Figure 8b) of fractal, however, the results also indicated that the fractal structures of conjugates were only accordant with the Eden model when the concentration of Cu (II) and Ag (I) increased. In addition, these results indicate that the combination of AFM and fractal dimension calculating provides a convenient and exact method to analyze the fractal dimension of chitosan and chitosan/metal ions aggregates.

## 4. Experimental

### *Material and Reagent*

Acetic acid, $NiCl_2$, $Cu(NO_3)_2$, $AgNO_3$ are all analytic reagent. X-ray diffractometer (XD-2, Peking Univ.). Chitosan (de-acetyl degree greater than 90%, viscosity less than 0.01pas, molecular weight is about $1.5\times10^6$ Daltons)(Bo'ao Biotechnology Corporation, Shanghai) dissolved in acetic acid solution (2%), and the final concentration of chitosan solution including 0.1 mg/ml, 1.0 mg/ml, and 2.5 mg/ml.

### *Sample preparation*

Chitosan solution (0.1 mg/ml) mixed with $Cu(NO_3)_2$ (1 mg/ml) and $AgNO_3$ (1 mg/ml) solution (V:V=1:1) to produce the conjugates of chitosan/metal ions. Then the prepared samples (about 10 μl) including chitosan solution and the conjugates of chitosan/metal ions were dropped on newly peeled mica, and then air dried.

As for the preparation of lyotropic liquid crystal (LLC) of chitosan, the electronegative mica was firstly treated with $NiCl_2$ solution to make mica electropositive, then about 5 μl chitosan/acetic acid (weight ratio=5%) solution (pH approximate 3) was dropped on electropositive mica, and then air-dried for AFM imaging. Figure 9 is the sketch illustration of preparation process of chitosan absorbed on mica.

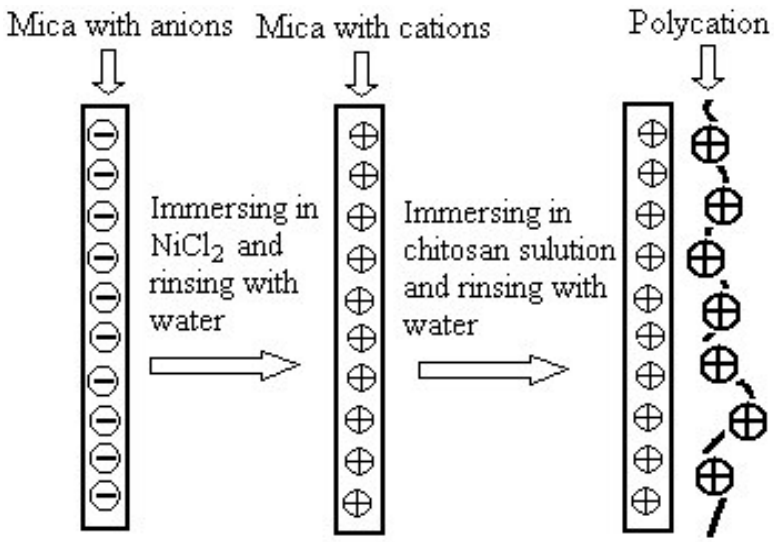


**Figure 9.** Sketch illustration of self-assembly strategy of chitosan on $NiCl_2$ treated mica.

*Atomic force microscope imaging*

The prepared samples were imaged at room temperature using an atomic force microscope (Autoprobe CP Research, Veeco) in the tapping mode. All images were acquired in air. The curvature radius of the silicon nitride tip was about 10 nm; the force constant was about 2.5 N/m and 3.2 N/m (manufacturer provided). All of the images were flattened with the provided software (IP 2.1 version) to eliminate low-frequency background noise in scanning direction. The calculation of the average rough (Ra) was auto-performed by AFM processing software, and the Ra is determined using the standard definition: $R_a = \frac{1}{N}\sum_{i=1}^{N}\left|Zi - \bar{Z}\right|$, where $\bar{Z}$ =mean z height. The Ra refers only to the included areas defined by a region group, with N given by the number of data points in the included areas.

*Fractal dimensional calculation*

Up to now, there are several methods to calculate the fractal dimension (D), however, the calculating formula: $D=(d^2+1)/(d+1)$, which was brought forward by Tokuyama and Kawasaki in 1984 [35], is more convenient, here $d$ is the Euclidean geometry dimension. The process of images processing including: noise signal removing, 256 pixel gray processing, two-value processing and fractal feature extracting. Then, the fractal dimension are calculated according to the formula $D=(d^2+1)/(d+1)$.

**Acknowledgements**

This research project is supported by the national natural science foundation of China (No. 60578025, 30230350, 30540420311).

## References


1. Nauta, K.; Miller, R.E. Nonequilibrium self-assembly of long chains of polar molecules in superfluid helium. *Science* **1999**, *283*, 1895-1897.
2. Serizawa, T.; Yamaguchi, M.; Akashi, M. Alternating Bioactivity of Polymeric Layer-by-Layer Assemblies: Anticoagulation vs Procoagulation of Human Blood. *Biomacromolecules* **2002**, *3*, 724-731.
3. Yi, H.; Wu, L.Q.; Sumner, J.J.; Gillespie, J.B.; Payne, G.F.; Bentley, W.E. Chitosan Scaffolds for Biomolecular Assembly: Coupling Nucleic Acid Probes for Detecting Hybridization. *Biotechnol. Bioeng*. **2003**, *83*, 646-652.
4. Cai, J.Y.; Chen, Y.; Xu, Q.C.; Chen, Y.; Zhao, T.; Wang, X.Y.; Xia, K. Atomic Force Microscope Imaging of the Aggregation of Mouse Immunoglobulin G Molecules. *Molecules* **2003**, *8*, 86-91.
5. Nilsson, K.P.R.; Rydberg, J.; Baltzer, L.; Inganas, O. Twisting macromolecular chains: Self-assembly of a chiral supermolecule from nonchiral polythiophene polyanions and random-coil synthetic peptides. *PNAS* **2004**, *101*, 11197-11202.
6. Li, X.; Wei, X.L.; Husson, S.M. Thermodynamic Studies on the Adsorption of Fibronectin Adhesion-Promoting Peptide on Nanothin Films of Poly(2-vinylpyridine) by SPR. *Biomacromolecules* **2004**, *5*, 869-876.
7. Chen, Y.; Cai, J.Y.; Xu, Q.C.; Chen, Z.W. Atomic force bio-analytics of polymerization and aggregation of phycoerythrin-conjugated immunoglobulin G molecules. *Mol. Immunol*. **2004**, *41*, 1247-1252.
8. Yi, H.; Wu, L.Q.; Ghodssi, R.; Rubloff, G.W.; Payne, G.F.; Bentley, W.E. A Robust Technique for Assembly of Nucleic Acid Hybridization Chips Based on Electrochemically Templated Chitosan. *Anal. Chem*. **2004**, *76*, 365-372.
9. Feng, Q.; Zeng, G.C.; Yang, P.H.; Wang, C.X.; Cai, J.Y. Self-assembly and characterization of polyelectrolyte complex films of hyaluronic acid/chitosan. Colloids and Surfaces A: *Physicochem Eng Aspects* **2005**, 257-258, 85-88.
10. Shih, W.M.; Quispe, J.D.; Joyce, G.F. A 1.7-kilobase single-stranded DNA that folds into a nanoscale octahedron. *Nature* **2004**, *427*, 618-621.
11. Dang, J.M.; Sun, D.D.; Shin-Ya, Y.; Sieber, A.N.; Kostuik, J.P.; Leong, K.W. Temperature-responsive hydroxybutyl chitosan for the culture of mesenchymal stem cells and intervertebral disk cells. *Biomaterials* **2005**, Aug 19, Epub ahead of print.
12. Haque, T.; Chen, H.; Ouyang, W.; Martoni, C.; Lawuyi, B.; Urbanska, A.; Prakash, S. Investigation of a new microcapsule membrane combining alginate; chitosan; polyethylene glycol and poly-L-lysine for cell transplantation applications. *Int. J. Artif. Organs* **2005**, *28*, 631-637.
13. Funakoshi, T.; Majima, T.; Iwasaki, N. Application of tissue engineering techniques for rotator cuff regeneration using a chitosan-based hyaluronan hybrid fiber scaffold. *Am. J. Sports Med*. **2005**, *33*, 1193-1201.
14. Zheng, C.H.; Liang, W.Q.; Li, F. Optimization and characterization of chitosan-coated alginate microcapsules containing albumin. *Pharmazie* **2005**, *60*, 434-438.
15. Matsumoto, T.; Kawai, M.; Masuda, T. Rheological properties and fractal structure of concentrated polyion complexes of chitosan and alginate. *Biorheology* **1993**, *30*, 435-441.

16. Zhang, C.; Qineng, P.; Zhang, H.J. Self-assembly and characterization of paclitaxel-loaded N-octyl-O-sulfate chitosan micellar system. Colloid Surface B: *Biointerfaces* **2004**, *39*, 69–75.
17. Liu, Y.J.; Li, Y.L.; Liu, S.C.; Li, J.; Yao, S.Z. Monitoring the self-assembly of chitosan/glutaraldehyde/ cysteamine/Au-colloid and the binding of human serum albumin with hesperidin. *Biomaterials* **2004**, *25*, 5725–5733.
18. Montembault, A.; Viton, C.; Domard, A. Rheometric study of the gelation of chitosan in a hydroalcoholic medium. *Biomaterials* **2005**, *26*, 1633-1643.
19. Lee, J.B.; Kim, D.J.; Choi, J.W.; Koo, K.K. Formation of a protein monomolecular layer by a combined technique of LB and SA methods. Colloid Surface B: *Biointerfaces* **2005**, *41*, 163-168.
20. Lvov, Y.; Onda, M.; Ariga, K. Ultrathin films of charged polysaccharides assembled alternately with linear polyions. *J. Biomater. Sci. Polym. Ed.* **1998**, *9*, 345-355.
21. Liu, H.; Mao, J.; Yao, K.; Yang, G.; Cui, L.; Cao, Y. A study on a chitosan-gelatin-hyaluronic acid scaffold as artificial skin in vitro and its tissue engineering applications. *J. Biomater. Sci. Polym. Ed.* **2004**, *15*, 25-40.
22. Ma, L.; Gao, C.; Mao, Z.; Zhou, J.; Shen, J.; Hu, X.; Han, C. Collagen/chitosan porous scaffolds with improved biostability for skin tissue engineering. *Biomaterials* **2003**, *24*, 4833-4841.
23. Dureja, H.; Tiwary, A.K.; Gupta, S. Simulation of skin permeability in chitosan membranes. *Int. J. Pharm.* **2001**, *213*, 193-198.
24. Hirano, S.; Tobetto, K.; Noishiki, Y. SEM ultrastructure studies of N-acyl- and N-benzylidene-chitosan and chitosan membranes. *J. Biomed. Mater. Res.* **1981**, *15*, 903-911.
25. Williams, N. Fractal Geometry Gets the Measure of Life's Scales. *Science* 1997, 276, 34.
26. Groebe, G.; Marsch, W.C.; Holzmann, H. The fractals theory and its significance for dermatology. *Hautarzt* **1990**, *41*, 388-391.
27. Losa, G.A.; Nonnenmacher, T.F. Self-similarity and fractal irregularity in pathologic tissues. *Mod. Pathol.* **1996**, 9, 174-182.
28. Maier, T. Chaos theory and complexity in psychiatry. *Psychother. Psychosom. Med. Psychol.* **1998**, *48*, 314-317.
29. Tang, S.; Ma, Y.; Sebastine, I.M. The fractal nature of Escherichia coli biological flocs. Colloids and Surfaces B: *Biointerfaces* **2001**, *20*, 211–218.
30. Mandelbrot, B.B.; Kol, B.; Aharony, A. Angular gaps in radial diffusion-limited aggregation: two fractal dimensions and nontransient deviations from linear self-similarity. *Phys. Rev. Lett.* **2002**, *88*, 055501.
31. Rout, D.K.; Barman, S.P.; Pulapura, S.K.; Gross, R.A. Cholesteric Mesophases Formed by the Modified Biological Macromolecules 3; 6-O-(Butyl Carbamate)-N-phthaloyl Chitosan. *Macromolecules* **1994**, *27*, 2945-2949.
32. Murray, S.B.; Neville, A.C. The role of pH; temperature and nucleation in the formation of cholesteric liquid crystal spherulites from chitin and chitosan. *Int. J. Biol. Macromol.* **1998**, *22*, 137-144.
33. Reiniger, M.; Basnar, B.; Friedbacher, G.; Schleberger, M. Atomic force microscopy of thin organic films on silicon in ultrahigh vacuum and under ambient conditions. *Surf. Interface Anal.* **2002**, *33*, 85-88.

34. Nittrnann, J.; Stanley, H.E. Tip splitting without interfacial tension and dendritic growth patterns arising from molecular anisotropy. *Nature* **1986**, *321*, 663.
35. Tokuyama, M.; Kawasaki, K. Fractal dimensions for diffusion-limited aggregation. *Phys. Lett. A.* **1984**, *100*, 337-340.